STRATEGY FOR LONG-TERM LIBRATION POINT ORBIT STATIONKEEPING IN THE EARTH-MOON SYSTEM

Thomas A. Pavlak[*] and Kathleen C. Howell[†]

Given the success of the first Earth-Moon libration point mission, ARTEMIS, it is likely that the Earth-Moon libration points will continue to be employed as platforms for space communications and scientific observations in the future. A long-term stationkeeping strategy for Earth-Moon libration point orbits is examined, one that does not require strict adherence to a baseline trajectory but retains the capability to meet a specific set of end-of-mission objectives for a planned lunar orbit insertion. The method is sufficiently general and is applied to both the ARTEMIS P1 and P2 trajectories in an ephemeris model.

INTRODUCTION

The Earth-Moon libration points have garnered increased interest in recent years. The current focus of attention is ARTEMIS, the first mission to incorporate the successful insertion of a spacecraft into orbit in the vicinity of an Earth-Moon libration point.[1,2] The first of two ARTEMIS spacecraft arrived near the Earth-Moon L_2 orbit in August 2010 and the second arrived in October 2010. Given the continuing success of both ARTEMIS probes, it is likely that the Earth-Moon libration points will be employed as platforms for space communications and scientific observations in the future. Orbits in the vicinity of the collinear libration points are generally unstable and must be maintained through regular stationkeeping maneuvers. From the experience with ARTEMIS in the Earth-Moon system, stationkeeping is required via a maneuver approximately once per week; and the path is very sensitive to any adjustments. Thus, to best meet future mission requirements in this dynamical regime, efficient, flexible stationkeeping algorithms requiring minimal human interaction are desired.

Due to the inherent orbital instability associated with libration point orbits, mission lifetimes are limited by the amount of stationkeeping propellant that is available. Depending on the mission requirements, a spacecraft may be required to adhere strictly to a baseline trajectory or, frequently, is required simply to remain in the vicinity of the libration point for a desired length of time. In either case, once the fuel supply is exhausted, a spacecraft is no longer able to maintain its orbit. For short-term stationkeeping, the stable invariant manifolds are useful to estimate the maneuver directions.[3] But, for long-term planning, the eventual libration point orbit departure requirements must also be considered during the mission design phase. In the Earth-Moon system, one end-of-

---

[*]Ph.D. Student, School of Aeronautics and Astronautics, Purdue University, Armstrong Hall of Engineering, 701 W. Stadium Ave., West Lafayette, Indiana 47907-2045.

[†]Hsu Lo Professor of Aeronautical and Astronautical Engineering, School of Aeronautics and Astronautics, Purdue University, Armstrong Hall of Engineering, 701 W. Stadium Ave., West Lafayette, Indiana 47907-2045. Fellow AAS; Associate Fellow AIAA.

mission option is to utilize unstable manifolds to depart the orbit and arrive in the lunar vicinity to be delivered to a planned lunar orbit in support of further communications and/or scientific activities.

If a continuous end-to-end solution is obtained, dynamical instabilities still prevent the reference path from being followed precisely and some form of orbit maintenance is required. Stationkeeping strategies based on Floquet theory offer one method to maintain a spacecraft in a libration point orbit and have been explored by Farquhar,[4] Breakwell et al.,[5] and many others.[6-8] A global search stationkeeping approach by Janes and Beckman[9] is designed to simply maintain a spacecraft in orbit for the next 1-2 revolutions downstream. It can be demonstrated that stable manifold directions are consistent with such short-term maintenance schemes.[3] While these approaches are an effective means of controlling short-term trajectory behavior, it is possible that, for some applications, the stationkeeping maneuvers could negatively affect the end-of-mission objectives. More recently, Grebow et al.[10] and Folta et al.[11] have used maneuvers to target back to a rigid baseline solution, or, at least, to target specific parameters downstream, but this general approach can result in higher stationkeeping costs and can create challenges when transitioning into the next mission phase.

Thus, the goal of this work is establishing a long-term stationkeeping strategy that does not require close tracking of a baseline trajectory but still meets a specific set of end-of-mission objectives, i.e., conditions at lunar arrival. This goal is achieved through the implementation of a multiple shooting algorithm that decomposes the trajectory into multiple segments and allows each station-keeping maneuver to target a set of terminal mission constraints, even for a distant end state. This strategy is sufficiently general and is potentially well-suited for automation. A reference solution construction procedure is outlined and demonstrated on the ARTEMIS P1 and P2 trajectories. The long-term stationkeeping strategy is employed with Monte Carlo simulations to demonstrate the process and approximates the stationkeeping ΔV costs for the ARTEMIS mission in an ephemeris model as an example.

SYSTEM MODELS

The ratio between the mass of the Moon and the mass of the Earth is large relative to other known planet-moon systems, thus, the motion of a spacecraft in the Earth-Moon region is often influenced heavily by both bodies simultaneously. Higher-fidelity effects such as lunar eccentricity and solar gravity also significantly impact the highly sensitive libration point orbits in the Earth-Moon system and should be included for stationkeeping analyses. However, it is often more practical to conduct preliminary mission design activities in lower-fidelity models. Periodic orbits and their associated manifolds are well-understood in the time-invariant circular restricted three-body problem (CR3BP) so it is convenient to use this dynamical model for preliminary reference trajectory design throughout this study. Furthermore, once a trajectory is designed in the CR3BP, it is generally straightforward to transition it to higher-fidelity models.[12, 13]

Circular Restricted Three-Body Problem

The dynamical environment that serves as the basis for the circular restricted three-body problem governs the motion of a "massless" spacecraft that is influenced by two gravity fields – in this case, the Earth and the Moon – that move in coplanar circular orbits about their barycenter. The model in the CR3BP is formulated in a rotating reference frame such that the positive x-axis direction is along the Earth-Moon line, the positive z-axis is oriented perpendicular to the orbital plane of the primaries, and the the y-axis completes the right-handed set. The coordinate system is centered at

the Earth-Moon barycenter. The mass parameter, μ, is defined as

$$\mu = \frac{m_M}{m_E + m_M} \tag{1}$$

where m_E is the mass of the Earth and m_M represents the mass of the Moon. The six-dimensional state vector is denoted $\boldsymbol{x} = \begin{bmatrix} x, y, z, \dot{x}, \dot{y}, \dot{z} \end{bmatrix}^T$, with bold symbols signifying vector quantities and position defined relative to the system barycenter. The second-order scalar equations of motion appear in the following form

$$\ddot{x} - 2\dot{y} - x = -\frac{(1 - \mu)(x + \mu)}{d_1^3} - \frac{\mu(x - 1 + \mu)}{d_2^3} \tag{2}$$

$$\ddot{y} + 2\dot{x} - y = -\frac{(1 - \mu)y}{d_1^3} - \frac{\mu y}{d_2^3} \tag{3}$$

$$\ddot{z} = -\frac{(1 - \mu)z}{d_1^3} - \frac{\mu z}{d_2^3} \tag{4}$$

with the scalar relative distances,

$$d_1 = \sqrt{(x + \mu)^2 + y^2 + z^2} \tag{5}$$

$$d_2 = \sqrt{(x - 1 + \mu)^2 + y^2 + z^2} \tag{6}$$

such that d_1 and d_2 are measured from the Earth to the spacecraft and the Moon to the spacecraft, respectively. For the computation of trajectories in either the CR3BP or ephemeris models, the second-order equations of motion are rewritten as a series of first-order differential equations in the form,

$$\dot{\boldsymbol{x}} = \boldsymbol{f}(t, \boldsymbol{x}) \tag{7}$$

where $\boldsymbol{x}$ is the six-dimensional state vector that contains both position and velocity information.

Libration Point Orbits and Associated Invariant Manifolds

When formulated in a rotating reference frame, the equations of motion in the CR3BP are autonomous and the solutions are time-invariant. Consequently, the five libration points, i.e., the equilibrium solutions to the equations of motion, are invariant as well and appear as constants relative to the rotating frame. Thus, the velocity and acceleration relative to the rotating frame at these points must be zero. The focus here are the orbits in the vicinity of the Earth-Moon L_1 and L_2 collinear libration points.

In the CR3BP, many periodic orbits in the vicinity of the collinear libration points are unstable and, consequently, possess stable and unstable invariant manifolds that offer numerous mission design applications. These manifolds are higher-dimensional surfaces that govern the asymptotic nature of the flow toward or away from a periodic libration point orbit. Such a flow structure allows transfers into and out of the periodic orbit without any maneuver. To generate manifold surfaces, a series of fixed points are selected around a periodic orbit. The monodromy matrix, M, is computed at each fixed point, $\boldsymbol{x}_i^*$, by integrating the state transition matrix (STM), $\phi(t, t_i)$, for one orbital period, P, i.e.,

$$M = \phi(t_i + P, t_i) \tag{8}$$

The eigenvalues of the monodromy matrix supply dynamical stability information. For a periodic orbit, the eigenvalues occur in reciprocal pairs and M possesses a determinant of one. When only two eigenvalues are real, the eigenvalues with the smallest and largest magnitudes correspond to the stable and unstable modes, respectively. To generate a manifold trajectory, a fixed point, x_i^*, is perturbed by some amount, d, along the eigenvector, ν, associated with the desired stable or unstable mode. For convenience, the eigenvector, ν, is normalized with respect to the position coordinates. Thus, the perturbed state, x, is written

$$x = x_i^* \pm d\,\nu \tag{9}$$

and numerically integrated. Stable manifold trajectories are generated using reverse-time integration while unstable manifold trajectories are constructed by employing forward-time integration. The collection of stable/unstable manifold trajectories from all fixed points around an orbit comprise the stable/unstable manifold surface corresponding to a given periodic libration point orbit. As an example, the stable (blue) and unstable (red) manifolds associated with a planar L_1 Lyapunov orbit appear in Figure 1.
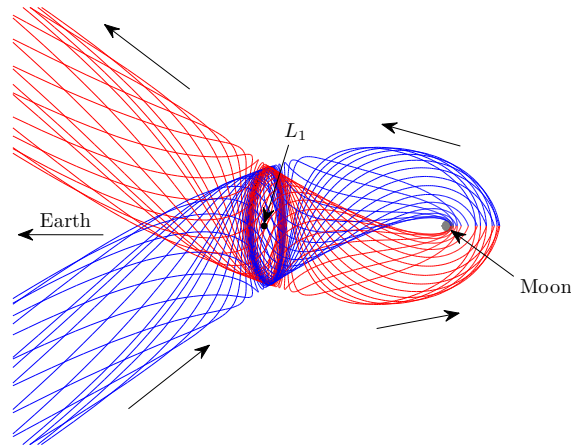
Figure 1. Invariant Manifold Associated with a Periodic L_1 Lyapunov Orbit

In this analysis, the invariant manifolds are used to support design for two primary purposes: 1) To construct essentially-free transfers from an L_2 orbit to an L_1 orbit via heteroclinic-type connections such that L_2 unstable manifolds flow into L_1 stable manifolds; and, 2) to design lost-cost transfers from an L_1 trajectory to the lunar vicinity using the unstable manifolds.

Ephemeris Model

Regardless of the stationkeeping scheme under investigation, the use of higher-fidelity dynamical modeling is required to more accurately predict actual mission ΔV costs. This added fidelity is particularly important near libration points in the Earth-Moon system given that lunar eccentricity and solar gravity can significantly affect trajectories in this regime. Thus, this analysis also includes a Moon-Earth-Sun point mass model incorporating the JPL DE405 ephemerides. Trajectories are integrated in a Moon-centered, inertial Earth J2000 reference frame using the familiar N-body

relative equations of motion,

$$\boldsymbol{r}_{qi}'' + \frac{\tilde{G}\left(m_i + m_q\right)}{r_{qi}^3}\boldsymbol{r}_{qi} = \tilde{G}\sum_{\substack{j=1 \\ j \neq i,q}}^{n} m_j \left(\frac{\boldsymbol{r}_{ij}}{r_{ij}^3} - \frac{\boldsymbol{r}_{qj}}{r_{qj}^3}\right) \tag{10}$$

where the vector $\boldsymbol{r}_{qj}$ represents the position of each perturbing body with respect to the central body, "q". These relative locations of the celestial bodies are delivered directly from DE405 ephemeris data. The vector $\boldsymbol{r}_{ij}$ then corresponds to the position of each perturbing body relative to the spacecraft, "i". The terms $\tilde{G}$ and m_k are the gravitational constant and the mass of body "k", respectively, expressed in dimensional units.

METHODOLOGY: NUMERICAL SCHEMES

The objective of a typical short-term stationkeeping strategy for libration point orbits is the development an algorithm that is sufficiently flexible to maintain a spacecraft in the vicinity of a libration point trajectory for some period of time without rigidly following a predetermined baseline trajectory. For long-term stationkeeping, the trajectory must be maintained for an extended period of time while retaining the capability to meet a set of precise end-of-mission orbital conditions. This goal is accomplished by, first, using a multiple shooting differential corrections algorithm to compute an initial, end-to-end virtual reference solution which is then employed as an initial guess to compute stationkeeping maneuvers. A stationkeeping algorithm is then required to target ahead, possibly all the way to a desired set of lunar arrival conditions.

Multiple Shooting Differential Corrections Algorithm

Once numerically integrated, the unstable nature of collinear libration point orbits causes the path to depart the vicinity of the orbit after only 1-2 revolutions. In other words, it is generally not possible to compute complex trajectories involving many libration point orbit revolutions, transfers, and terminal conditions using a single numerically integrated trajectory from given initial conditions. However, decomposing the trajectory into multiple segments significantly reduces the dynamical sensitivities associated with each arc and allows libration point orbits comprised of any number of revolutions to be generated through the use of a multiple shooting differential corrections algorithm. These numerical schemes also allow constraints along the path as well as at the end points. Multiple shooting algorithms are extremely powerful tools and, in this analysis, are critical to generating reference solutions and computing maneuvers in the long-term stationkeeping approach.

The general framework for a multiple shooting scheme appears in Figure 2 with a discontinuous initial guess in Figure 2(a) and the converged, continuous trajectory in Figure 2(b). The trajectory is discretized into n "patch points" that are associated with $n-1$ arcs. The vector, $\boldsymbol{x_i}$, represents the six-dimensional state at each patch point (where each trajectory arc originates) and the integration time along each segment is denoted as T_i. The epoch at each patch point, necessary for application in a time-dependent ephemeris model, are labeled τ_i. The final integrated state along each segment, that is, $\boldsymbol{x}_i^t\left(\boldsymbol{x}_{i-1}, T_{i-1}\right)$, is expressed in a shortened notation as $\boldsymbol{x}_i^t$. Note that the trajectory, as represented via a series of segments or arcs, is discontinuous, possibly in all seven states, at each patch point.

Various implementations of differential corrections schemes are available. In this analysis, a constraint-variable algorithm is employed.[12] Thus, to compute a continuous trajectory that also
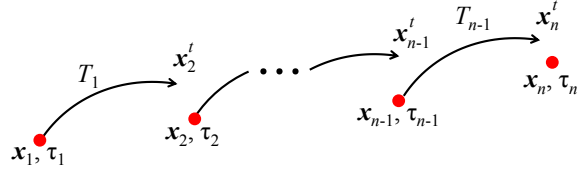
(a) Initial Guess
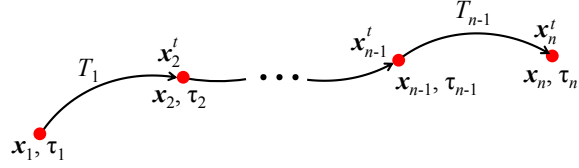
(b) Converged

Figure 2. Multiple Shooting Schematic

satisfies any desired end constraints, it is first necessary to define the free variables in the problem. To implement multiple shooting in an ephemeris model, the state at each patch point, the integration time along all segments, and the epochs of the internal patch points are all allowed to vary. These elements are combined into a free variable vector, $\boldsymbol{X}$. For a trajectory consisting of n patch points, the vector $\boldsymbol{X}$ has length $8n - 3$ and is ordered as follows,

$$\boldsymbol{X} = \begin{bmatrix} \boldsymbol{x}_1 \\ \vdots \\ \boldsymbol{x}_n \\ T_1 \\ \vdots \\ T_{n-1} \\ \tau_2 \\ \vdots \\ \tau_{n-1} \end{bmatrix} \tag{11}$$

The objective in a multiple shooting algorithm is the elimination of discontinuities in position, velocity, and time between the segments along the path and satisfaction of any additional constraints on the end points of the trajectory as appropriate. For the ARTEMIS examples that appear later in this paper, the following end point constraints are included (in addition to the continuity constraints at the internal patch points):

1. Fixed initial position
2. Final altitude at lunar arrival ($h_f = h_{f,desired}$)
3. Final patch point is a periapsis with respect to the Moon ($\boldsymbol{r}_f \cdot \boldsymbol{v}_f = 0$)
4. Final epoch at lunar arrival ($\tau_f = \tau_{f,desired}$)

Combining the continuity and end point requirements into a single constraint vector, $\boldsymbol{F}(\boldsymbol{X}) = \boldsymbol{0}$,

6

of length $7n - 2$ yields,

$$
F\left(X\right) = \begin{bmatrix} x_2^t - x_2 \\ \vdots \\ x_n^t - x_n \\ (\tau_1 + T_1) - \tau_2 \\ \vdots \\ (\tau_{n-2} + T_{n-2}) - \tau_{n-1} \\ x_{1,1:3} - x_{1,1:3,desired} \\ h_f - h_{f,desired} \\ r_f \cdot v_f \\ (\tau_{n-1} + T_{n-1}) - \tau_{f,desired} \end{bmatrix} = 0
\tag{12}
$$

To update the design vector, X, the Jacobian matrix, $DF\left(X\right)$, is required to relate changes in constraints to changes in the free variables, i.e.,

$$
DF\left(X\right) = \frac{\partial F\left(X\right)}{\partial X}
\tag{13}
$$

Since there are more free variables than constraints, a converged solution, X^*, is produced via an iterative first-order minimum-norm update equation,

$$
X^{j+1} = X^j - DF\left(X^j\right)^T \left[DF\left(X^j\right) DF\left(X^j\right)^T\right]^{-1} F\left(X^j\right)
\tag{14}
$$

Although the process is iterative, convergence is generally quick.

Computing a Reference Solution

Before a long-term stationkeeping strategy (and some short-term approaches) can be implemented, a reference solution, i.e., an initial guess for the numerical algorithm, must first be computed. The initial step in computing an end-to-end reference trajectory is to generate a suitable initial guess for the multiple shooting differential corrector. The design of the initial guess is, of course, reliant upon the type of mission under investigation. As noted previously, both of the ARTEMIS spacecraft are, fundamentally, libration point orbiters that enter lunar orbit at the end of their respective missions. Thus, the circular restricted three-body problem is ideally suited for initial guess design given the relative simplicity of computing periodic orbits and their associated invariant manifolds compared to more complex, higher-fidelity models. The reference solution design process is discussed briefly here, but is later examined in detail for each application to the ARTEMIS trajectories.

First, planar Lyapunov orbits of desired amplitudes are computed in the CR3BP and discretized into patch points. When multiple revolutions of a libration point orbit are required, the patch points from the computed Lyapunov orbit are simply stacked for the specified number of revolutions. If transfers between the orbits are required, unstable manifolds are propagated in forward time from the "departure orbit" and stable manifolds are propagated in reverse time from the "arrival orbit." An initial guess for the heteroclinic connection phase of the mission is obtained by selecting a near-tangent intersection between an unstable and stable manifold trajectory and discretizing the paths. To design the lunar approach leg of the mission, unstable manifolds are generated from the final

libration point orbit and the manifold trajectory which best approximates the desired lunar arrival condition (altitude, prograde/retrograde, etc.) is selected and decomposed into segments and patch points as well.

This initial set of patch points is then converged in the circular restricted three-body problem using the multiple shooting algorithm described in the previous section. Note, however, that it is not necessary to include the variables and constraints associated with the epoch times since the CR3BP is time-invariant. In the higher-fidelity analysis, the patch points from the converged CR3BP reference solution are transformed into a Moon-centered Earth J2000 reference frame and reconverged in the ephemeris model using multiple shooting.[12]

STATIONKEEPING STRATEGIES

Regardless of the approach, the fundamental objective of any stationkeeping algorithm is to design maneuvers that maintain a spacecraft orbit for some desired length of time. Such stationkeeping methods are particularly important for missions like ARTEMIS, since the spacecraft will depart their respective orbits relatively quickly if not regularly maintained. There are a variety of approaches to orbit maintenance in the Earth-Moon system, but all can be generally classified as either short-term or long-term stationkeeping strategies.

Short-Term Stationkeeping

The goal of short-term stationkeeping algorithms are, generally speaking, to maintain a spacecraft in a libration point orbit for the next 1-2 revolutions downstream. The focus is on controlling the trajectory in the near-term while end-of-mission constraints are addressed only when the mission nears its conclusion. A variety of short-term approaches have been examined and/or implemented.[3] A number of these strategies were explored for application to the ARTEMIS mission and, operationally, stationkeeping maneuvers were planned using an optimization process designed to keep the spacecraft in orbit for 1-2 revolutions into the future.[11] A typical ARTEMIS stationkeeping maneuver is represented in black in Figure 3. Despite the fact that these maneuvers were designed

(a)   (b)
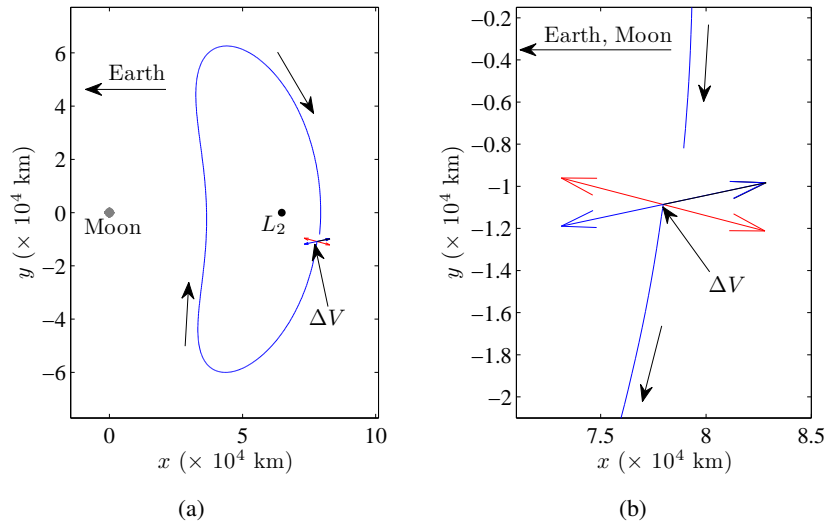
Figure 3. Alignment between ΔV Direction and the Stable Eigenvector

using solely a gradient-based optimizer, a recent research investigation has demonstrated that the ΔV direction (black) actually aligns closely with a direction parallel to the stable eigenvector (blue) for each of the ARTEMIS stationkeeping maneuvers; a sample maneuver (black) is depicted with the stable (blue) and unstable (red) eigenvectors in the zoomed view in Figure 3(b). A summary of the relative maneuver directions appears in Folta et al.[3] Essentially, the optimizer independently produces maneuvers that are generally consistent with the stable direction. Algorithms incorporating the stable manifold direction into the maneuver planning are also under development. The eigen-information is obtained by integrating the ephemeris trajectory for one revolution and an approximate monodromy matrix is obtained via finite differencing. The use of Lyapunov exponents for generating stability information in this application is also under investigation.[14]

Long-Term Stationkeeping Strategy

As stated previously, the goal for long-term stationkeeping is a strategy that does not require a baseline trajectory but can still meet a specific set of end-of-mission objectives, i.e., conditions at lunar orbit insertion. A multiple shooting stationkeeping algorithm is applied in conjunction with an artificial reference solution to conduct maneuver planning activities. Each time a maneuver is designed, the remaining leg along a reference trajectory is used as an initial guess in a multiple shooting algorithm to target pre-specified conditions at lunar arrival. Effectively, the reference solution is updated as each maneuver is planned as well. This global-type approach ensures that planned maneuvers do not disrupt the remaining trajectory arcs or negatively impact the end-of-mission goals.

Since the original reference solution is entirely continuous in position and velocity (within numerical tolerances), the cost of stationkeeping this "baseline" trajectory is essentially zero. In reality, however, the spacecraft does not follow the reference solution exactly due to errors associated with modeling, navigation, and maneuver execution. Therefore, actual mission stationkeeping costs are estimated by inserting random, normally-distributed position and velocity errors at each maneuver location. For these simulations, 1σ navigation errors of 1 km and 1 cm/s are incorporated.[11] A 1% hot/cold simulated maneuver execution error is applied to each stationkeeping maneuver as well. Monte Carlo simulation is employed to estimate the average total ΔV costs for a given mission design. In summary, the complete long-term stationkeeping algorithm is applied in terms of the following steps:

1. Obtain reference solution in desired dynamical model
2. Apply simulated navigation errors to initial state
3. Integrate from initial point to first stationkeeping maneuver location
4. Compute maneuver using remaining leg of reference solution as initial guess
5. Apply simulated navigation and maneuver execution errors
6. Integrate to next stationkeeping maneuver location
7. Repeat steps 4-6 until final stationkeeping maneuver is performed
8. Apply simulated navigation and maneuver execution errors
9. Integrate to end-of-mission condition (lunar arrival, etc.)

The long-term strategy is illustrated for an L_2 libration point orbit mission as modeled in the CR3BP in Figure 4. The asterisk denotes the first stationkeeping maneuver, the blue line represents the

trajectory that trails the vehicle, and the black line is the remaining portion along the reference solution that will be used to compute the next stationkeeping maneuver.
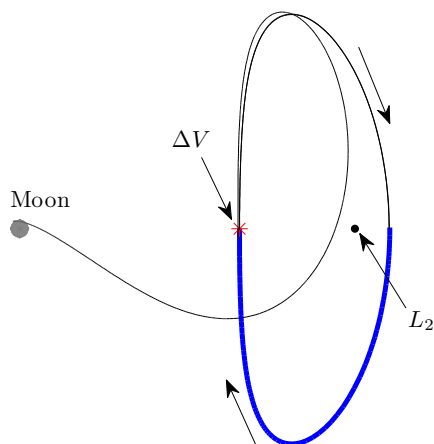
Figure 4. Long-Term Stationkeeping Example

APPLICATION TO THE ARTEMIS MISSION

The ARTEMIS P1 and P2 trajectories were both designed so that the spacecraft would spend multiple revolutions in orbit near the Earth-Moon L_2 and/or L_1 libration points before eventually entering lunar orbit. The complexity and dynamical instability of these trajectories make them ideal applications for a long-term stationkeeping strategy. The purpose of the following examples is to illustrate ARTEMIS-like trajectories that can be reconstructed and maintained using the long-term stationkeeping techniques detailed previously. For both the P1 and P2 trajectories, the initial guess for the reference solutions are constructed using planar Lyapunov orbits with y-amplitudes approximately equal to those used in the design of the actual mission. The initial states and epochs for the two trajectories originate from L_2 orbit insertion information based on actual orbit determination data. Additionally, in this analysis, stationkeeping maneuvers are implemented at all rotating xz-plane crossings, i.e., approximately once per week. Note that the P1 and P2 examples reflect the ARTEMIS mission design as of August 2010.

ARTEMIS P1 Trajectory

For purposes of this analysis, the Earth-Moon libration point orbit phase for the ARTEMIS P1 trajectory begins with insertion into an L_2 Lissajous orbit on August 22, 2010. After remaining in the L_2 vicinity for approximately 131 days, the spacecraft transitions to an L_1 Lissajous orbit for 85 days before departing for a retrograde lunar arrival at a periapsis altitude of 1500 km on April 9, 2011.

To design the initial guess for the ARTEMIS P1 trajectory, L_1 and L_2 Lyapunov orbits of the appropriate y-amplitudes of ~59,000 km and ~64,000 km, respectively, are computed in the circular restricted three-body problem. To simplify the computation of heteroclinic connections between the two orbits, a differential corrections process is used to compute two orbits with an equal energy level (Jacobi constant). These Lyapunov orbits are plotted in Figure 5. The orbits are discretized

and their patch points are stacked to produce the desired number of revolutions about each libration point. The initial guess for the ARTEMIS P1 reference solution utilizes seven stacked revolutions about L_2 and four about L_1. The transfer from the L_2 to the L_1 orbit is designed by generating
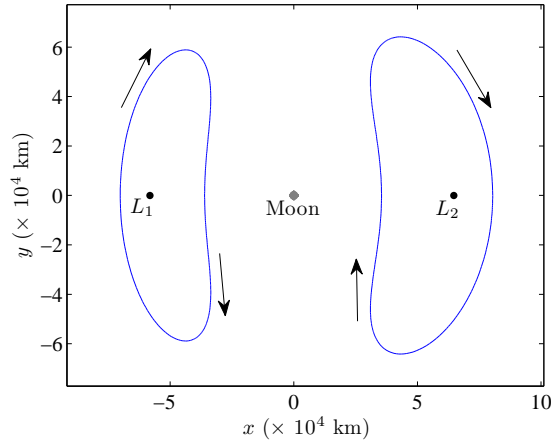
Figure 5. L_1 and L_2 **Lyapunov Orbits in the CR3BP for ARTEMIS P1 Trajectory**

unstable L_2 Lyapunov manifolds (red) in forward time and stable L_1 Lyapunov manifolds (blue) in reverse time as illustrated in Figure 6(a). The near-tangent manifold intersection displayed in Figure 6(b) is selected as the initial guess for the heteroclinic transfer phase of the trajectory. After approximately four revolutions in the L_1 orbit, descent to lunar orbit commences. The departure

(a)

(b)
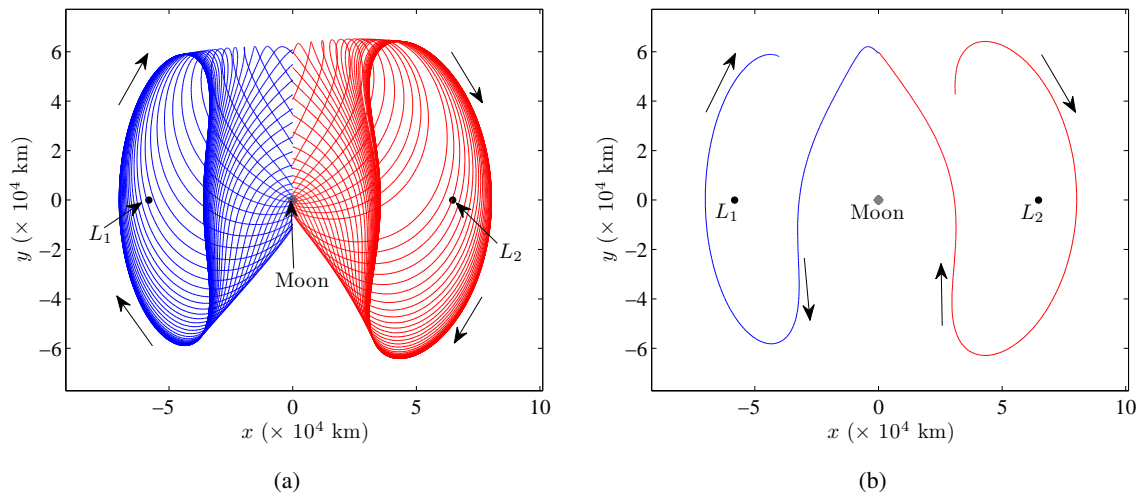
Figure 6. **Intersection of Unstable L_2 and Stable L_1 Manifolds for ARTEMIS P1 Trajectory**

from the L_1 orbit to achieve the desired lunar arrival conditions is initially planned in this analysis by integrating the unstable L_1 Lyapunov manifolds to the lunar vicinity as illustrated in Figure 7(a). Clearly, many feasible lunar arrival options exist; all arrive at different altitudes and times. The manifold trajectory that appears in Figure 7(b) is selected since it produces a retrograde arrival at roughly the required 1500 km lunar altitude. The manifold transfer legs are also discretized and

11
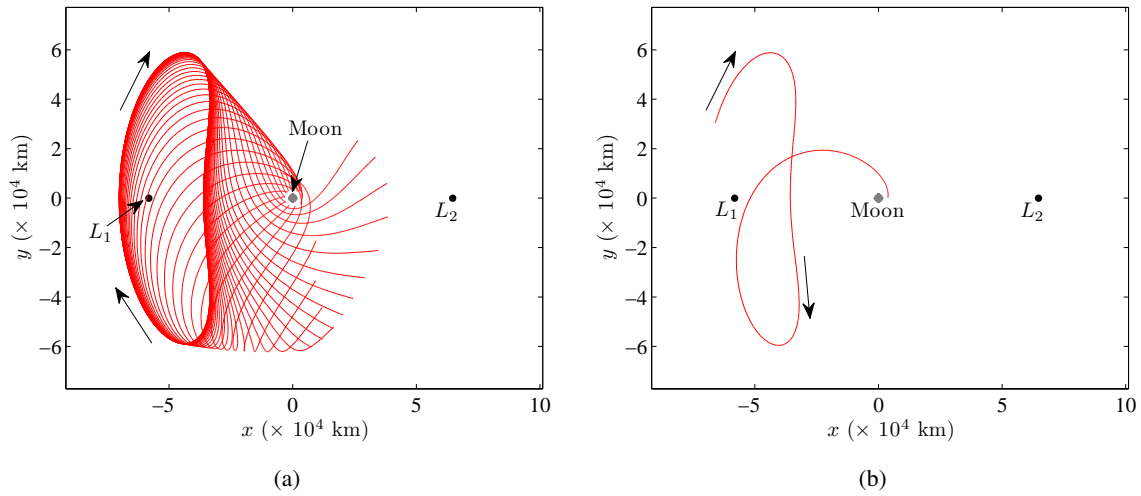
Figure 7. Unstable L_1 Manifolds for Lunar Arrival for ARTEMIS P1 Trajectory

combined with the libration point orbit patch points and the known L_2 Lissajous orbit insertion condition to form the initial guess for the ARTEMIS P1 reference solution in the CR3BP as combined and represented in Figure 8. The asterisks denote the patch points for the differential corrections process. Note that the entire initial guess is planar except for the initial state. The multiple shooting scheme can accommodate different types of arcs and performs quite efficiently. The algorithm con-
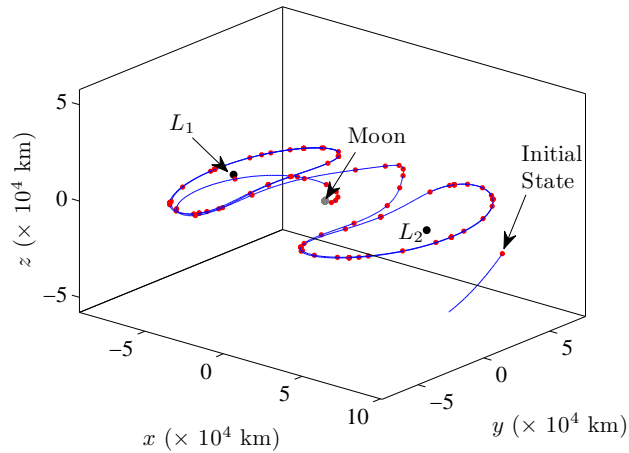
Figure 8. Initial Guess for ARTEMIS P1 Reference Solution in the CR3BP

verges successfully to an ARTEMIS P1 reference solution in the CR3BP that satisfies all end point constraints and appears in Figure 9. While only periapsis altitude and time are targeted at lunar arrival in this analysis, it is straightforward to implement additional constraints such as flight path angle, inclination, etc. The significant z-amplitude excursion in the L_2 and L_1 Lissajous orbits is a result of fixing the position of the out-of-plane initial state in the differential corrections algorithm. A higher-fidelity reference solution is readily obtained by transforming the CR3BP patch points to a Moon-centered Earth J2000 reference frame and reconverging the trajectory in a multiple shoot-

12

ing algorithm that incorporates a Moon-Earth-Sun point mass ephemeris model. The converged P1 ephemeris trajectory appears nearly identical to the CR3BP solution. This result in the ephemeris model serves as a reference solution for analysis. Operationally, a new reference path can be determined after every orbit determination solution is obtained.
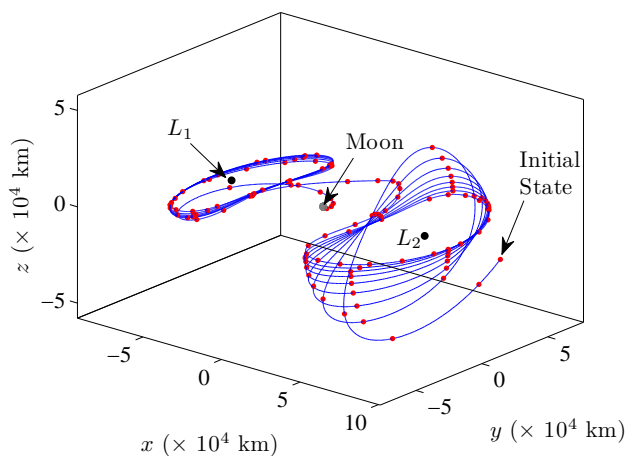
Figure 9. Converged ARTEMIS P1 Reference Trajectory in the CR3BP

The average total ΔV cost associated with stationkeeping the ARTEMIS P1 spacecraft is estimated using the long-term stationkeeping strategy and a Monte Carlo simulation comprised of 500 trials. Stationkeeping maneuvers are incorporated at all xz-plane crossings for a total of 32 stationkeeping maneuvers per trial as depicted in Figure 10. The final desired 1500 km x 18,000 km (altitude) lunar orbit is illustrated in red. In this simulation, the average total cost to maintain the sample ARTEMIS P1 spacecraft during its 7.5 month trajectory is determined to be 14.40 m/s, or approximately 45.0 cm/s per maneuver. These results are consistent with previous estimates of stationkeeping costs for libration point orbits in the Earth-Moon system in previous studies conducted by Grebow et al.[10] and Folta et al.[11] incorporating similar error levels. Note that stationkeeping costs for the actual ARTEMIS P1 trajectory are lower than the results presented here due to the fact that the actual navigational uncertainties during operation were significantly smaller than the estimates used in this analysis.[3]

ARTEMIS P2 Trajectory

The ARTEMIS P2 path differs from that of P1, but the reference solution design procedure is very similar. For this study, the Earth-Moon libration point orbiting phase of the P2 design begins with insertion on the L_2 side on October 3, 2010. Unlike its counterpart, the ARTEMIS P2 spacecraft does not complete a full revolution about L_2, but rather immediately transfers to the L_1 side where it remains in a Lissajous orbit for approximately 154 days. The P2 trajectory departs the L_1 orbit consistent with the original design as of August 2010, and the spacecraft is delivered to a prograde lunar arrival at a periapsis altitude of 1500 km on April 19, 2011.

The design strategy requires, first, an initial guess for a reference solution, given the desired arrival conditions into the lunar vicinity. The design of the initial guess for the ARTEMIS P2 reference solution begins with an L_1 Lyapunov orbit in the circular restricted three-body problem

13
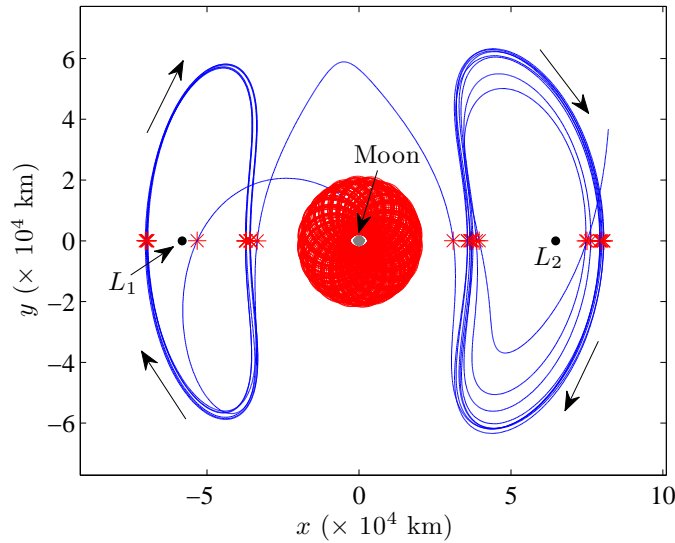
Figure 10. Stationkeeping Maneuver Locations for the ARTEMIS P1 Trajectory

that is defined such that the y-amplitude is $\sim$71,500 km. A differential corrections scheme is used to generate an L_2 Lyapunov orbit with a Jacobi constant of equal value. The two Lyapunov orbits are plotted in Figure 11. For the P2 trajectory, the L_1 orbit is discretized into patch points and stacked for ten revolutions. The invariant manifolds are again exploited to produce trajectory arcs to initially
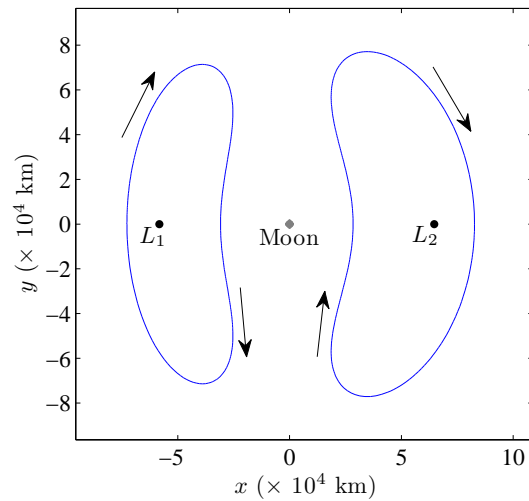
Figure 11. L_1 and L_2 Lyapunov Orbits in the CR3BP for ARTEMIS P2 Trajectory

represent the L_2-to-L_1 transfer from one side of the Moon to the other as viewed from Earth. The unstable L_2 Lyapunov manifolds (red) and stable L_1 Lyapunov manifolds (blue) are illustrated in Figure 12(a). The near-tangent intersection of two manifold trajectories in Figure 12(b) form the initial guess for the transfer phase of the P2 trajectory. The departure from the L_1 orbit to the lunar vicinity is developed from the unstable manifolds associated with the L_1 libration point orbit; the

14
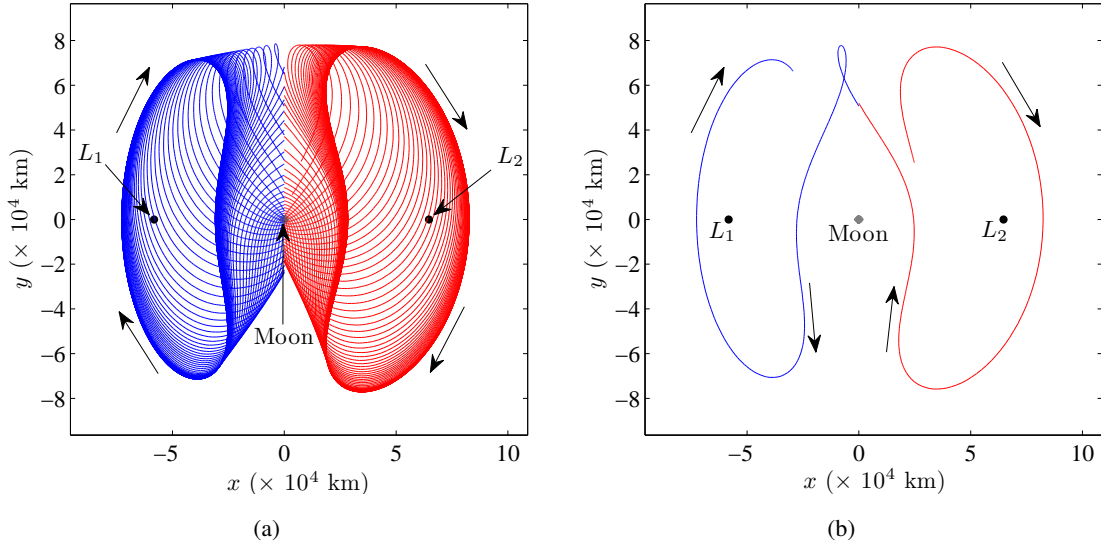
Figure 12. Intersection of Unstable L_2 and Stable L_1 Manifolds for ARTEMIS P2 Trajectory

manifolds are propagated until lunar arrival as plotted in Figure 13(a). The manifold trajectory arc in Figure 13(b) is selected since it produces a prograde lunar arrival near the required 1500 km altitude. The arrival conditions need not be exact for the first approximation.
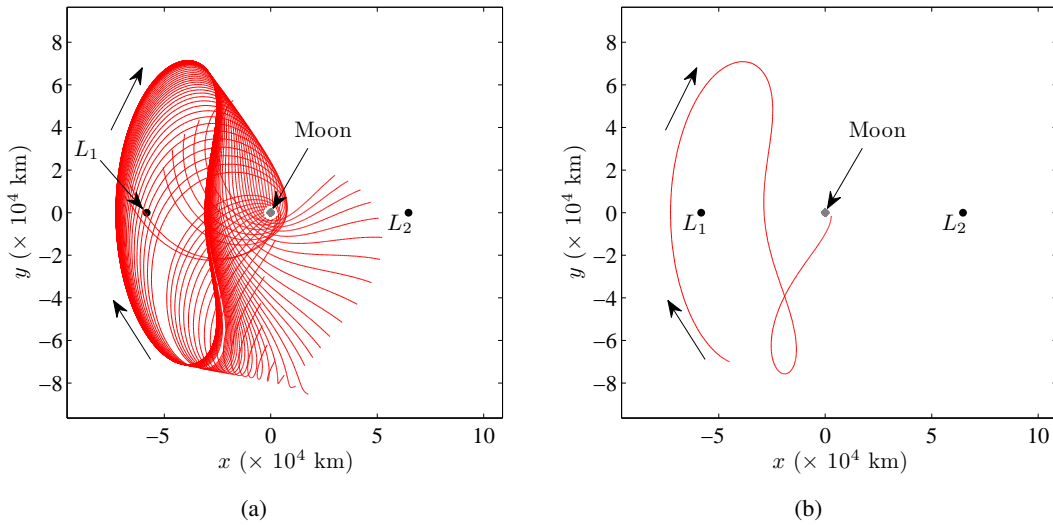
Figure 13. Unstable L_1 Manifolds for Lunar Arrival for ARTEMIS P2 Trajectory

Given a suitable set of arcs to represent the path, all arcs are now blended to yield a converged path. Combining the discretized L_2-L_1 transfer and L_1 unstable manifold trajectory that leads directly to lunar arrival with the stacked L_1 Lyapunov patch points produces the initial condition for the ARTEMIS P2 reference solution that appears in Figure 14. The multiple shooting algorithm

15
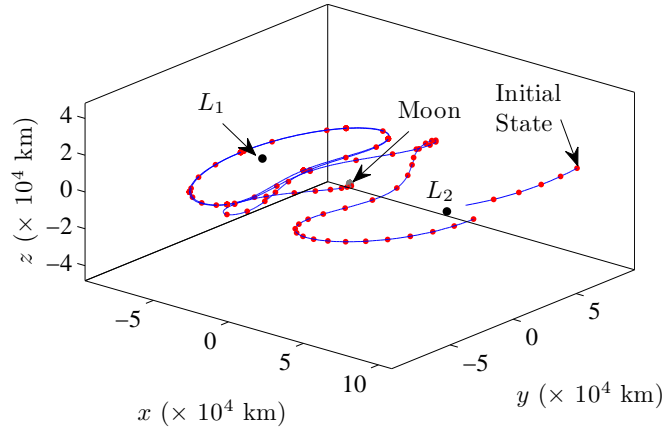
Figure 14. Initial Guess for ARTEMIS P2 Reference Solution in the CR3BP

uses these points and converges to a continuous CR3BP trajectory displayed in Figure 15 with a prograde lunar arrival at the required time with a 1500 km periapsis altitude. Similar to the P1 trajectory, the CR3BP ARTEMIS P2 reference solution is reconverged in a higher-fidelity Moon-Earth-Sun ephemeris model to improve that accuracy of the P2 stationkeeping analysis.
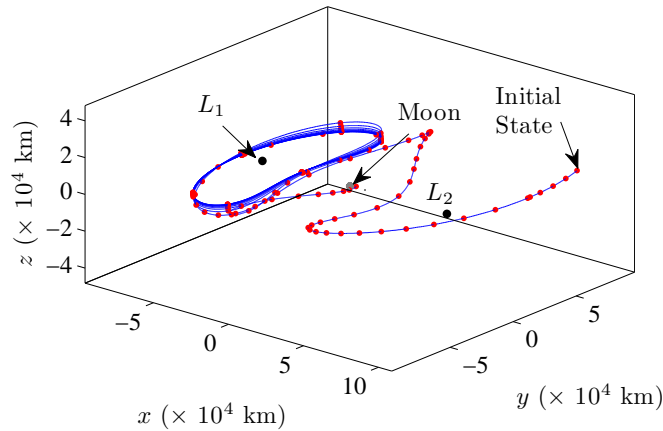
Figure 15. Converged ARTEMIS P2 Reference Trajectory in the CR3BP

The long-term stationkeeping strategy is sufficiently general and is applied to the ARTEMIS P2 trajectory by simply loading the P2 reference solution at the beginning of the algorithm. A 500-trial Monte Carlo simulation is conducted for P2 as well and the stationkeeping maneuvers are again constrained to occur at xz-plane crossings for a total of 27 maneuvers per trial. The maneuver locations as well as the final 1500 km x 18,000 km prograde lunar orbit (red) appear in Figure 16. The average total stationkeeping cost per trial is 13.18 m/s which equates to 48.8 cm/s per maneuver, again consistent with results from previous studies in this regime. The ΔV cost for stationkeeping the actual ARTEMIS P2 trajectory were significantly lower than those predicted here, given the overly-conservative estimates of the navigational uncertainties utilized in this analysis.

16
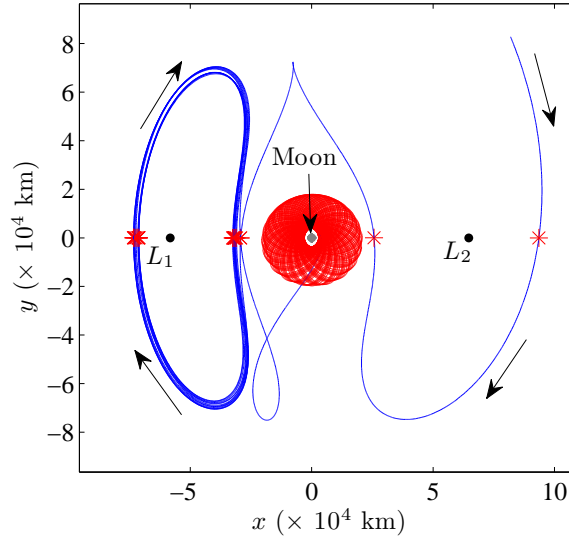
Figure 16. Stationkeeping Maneuver Locations for the ARTEMIS P2 Trajectory

CONCLUSION

The ARTEMIS mission underscores the value of numerical methods that allow for flexibility during the intermediate phases of a mission but still enable the trajectory to satisfy precise end-of-mission constraints. The long-term stationkeeping strategy seeks to address both issues. By joining many different trajectory segments together, each stationkeeping maneuver is able to target the set of terminal conditions as well as any path constraints; the process ensures that each planned maneuver does not negatively impact the end goals of the mission. The shortened time-scales in the Earth-Moon system dictate that libration point orbit stationkeeping maneuvers be performed approximately once every 7 days. Thus, the long-term stationkeeping strategy has operational advantages as well, given that it is generally robust and potentially well-suited for automation.

The ARTEMIS P1 and P2 trajectories are employed in this analysis to demonstrate the design of reference solutions using multiple shooting and the application of the long-term stationkeeping strategy to complex missions in the Earth-Moon system. Monte Carlo simulations incorporating random navigation and maneuver execution errors are conducted and produce average total mission ΔV costs that are on par with previous Earth-Moon libration point stationkeeping studies.

ACKNOWLEDGMENTS

REFERENCES

[1] M. Woodard, D. Folta, and D. Woodfork, "ARTEMIS: The First Mission to the Lunar Libration Points," *21st International Symposium on Space Flight Dynamics*, Toulouse, France, September 28-October 2, 2009.

[2] V. Angelopoulus, "The THEMIS Mission," *Space Science Reviews*, Vol. 141, No. 1-4, 2008, pp. 5–34.

[3] D. Folta, M. Woodard, and D. Cosgrove, "Stationkeeping of the First Earth-Moon Libration Orbiters: The ARTEMIS Mission," *AAS/AIAA Astrodynamics Specialist Conference*, Girdwood, Alaska, July 31 - August 4, 2011. Paper No. AAS 11-515.

[4] R. Farquhar, "The Utilization of Halo Orbits in Advanced Lunar Operations," NASA X-551-70-449, GSFC, Greenbelt, Maryland, 1970.

[5] J. Breakwell, A. Kamel, and M. Ratner, "Station-Keeping for a Translunar Communications Station," *Celestial Mechanics*, Vol. 10, No. 3, 1974, pp. 357–373.

[6] C. Simó, G. Gómez, J. Libre, R. Martínez, and J. Rodríguez, "On the Optimal Station Keeping Control of Halo Orbits," *Acta Astronautica*, Vol. 15, No. 6/7, 1987, pp. 391–397.

[7] K. C. Howell and T. M. Keeter, "Station-Keeping Strategies for Libration Point Orbits: Target Point and Floquet Mode Approaches," *Proceedings of the AAS/AIAA Spaceflight Mechanics Conference 1995*, Advances in the Astronautical Sciences, Vol. 89, R. Proulx, J. Liu, P. Seidelmann, and S. Alfano (editors), 1995, pp. 1377-1396.

[8] G. Gómez, K. Howell, J. Masdemont, and C. Simó, "Station-Keeping Strategies for Translunar Libration Point Orbits," *Proceedings of the AAS/AIAA Spaceflight Mechanics Conference 1998*, Advances in the Astronautical Sciences, Vol. 99, Part II, J. Middour, L. Sackett, L. D'Amario, and D. Byrnes (editors), 1998, pp. 949-967.

[9] L. Janes and M. Beckman, "Stationkeeping Maneuvers for the James Webb Space Telescope," *Goddard Flight Mechanics Symposium*, Greenbelt, Maryland, 2005.

[10] D. Grebow, M. Ozimek, K. Howell, and D. Folta, "Multibody Orbit Architectures for Lunar South Pole Coverage," *Journal of Spacecraft and Rockets*, Vol. 45, No. 2, 2008, pp. 344–358.

[11] D. Folta, T. Pavlak, K. Howell, M. Woodard, and D. Woodfork, "Stationkeeping of Lissajous Trajectories in the Earth-Moon System with Applications to ARTEMIS," *20th AAS/AIAA Space Flight Mechanics Meeting*, San Diego, California, February 14-17, 2010. Paper No. AAS 10-113.

[12] T. Pavlak, "Mission Design Applications in the Earth-Moon System: Transfer Trajectories and Station-keeping," M.S. Thesis, Purdue University, West Lafayette, Indiana, 2010.

[13] B. Marchand, S. Scarritt, T. Pavlak, and K. Howell, "Investigation of Alternative Return Strategies for Orion Trans-Earth Injection Design Options," *20th AAS/AIAA Space Flight Mechanics Meeting*, San Diego, California, February 14-17, 2010. Paper No. AAS 10-128.

[14] C. Short, K. Howell, and X. Tricoche, "Lagrangian Coherent Structures in the Restricted Three-Body Problem," *21st AAS/AIAA Space Flight Mechanics Meeting*, New Orleans, Louisiana, February 13-17, 2011. Paper No. AAS 11-250.